



Animal Bone Meal as new recyclable and ecological catalyst for the oximes Synthesis in solvent-Free Conditions

M. Ait Taleb^{1,2}, R. Mamouni^{1*}, N. Saffaj¹, A. Mouna², M.L. Taha²,
A. Benlhachemi³, B. Bakiz³, M. Ezahri³, S. Villain⁴

¹Equipe de Matériaux Catalyse et Valorisation des Ressources Naturelles, Faculté des Sciences, Université Ibn Zohr, Agadir, Maroc.

²Equipe de Chimie Bio-Organique Appliquée, Faculté des Sciences, Université Ibn Zohr, Agadir, Maroc.

³Laboratoire Matériaux et Environnement LME, Faculté des Sciences, Université Ibn Zohr, Agadir, Maroc.

⁴Institut Matériaux Microélectronique et Nanosciences de Provence, Aix Marseille Université, CNRS, Université de Toulon, IM2NP UMR 7334, 83957, La Garde, France.

Received 18 Jan 2016, Revised 06 Mar 2016, Accepted 15 Mar 2016

*Corresponding author. E-mail: rachidmamouni1@gmail.com (R. Mamouni); Phone: +212662048422, Fax: +212528220100.

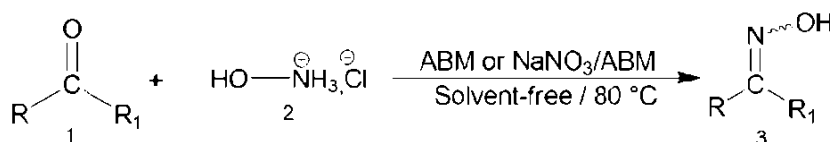
Abstract

In this present study, the transformation of ketones or aldehyde to the corresponding oximes was efficiently achieved using Animal Bone Meal alone and modified Animal Bone Meal with sodium nitrate as two new heterogeneous catalysts which respect the environment and does not cause any toxicity. These heterogeneous catalysts exhibited excellent catalytic activity under free-solvent conditions. The salient benefits of this method rely on various factors namely: a mildness of the reaction conditions, short reaction times, operational simplicity, high chemoselectivity, low cost and reusability several times with only a slight loss of activity.

Keywords: Oximes, Animal Bone Meal, heterogeneous catalysts, recyclable catalyst

1. Introduction

The oximes of ketones and aldehydes may be found in numerous pharmaceutical and agrochemical agents with a diverse spectrum of biological proprieties [1-5]. They are also used in organic synthesis as synthetic intermediates [6-12]. For several decades many synthetic methods have been developed for their synthesis such as NaOH, basic Al₂O₃, CaO, ZnO, FeCl₃, TiO₂/SO₄²⁻, Na₂SO₄, ionic liquids, pyridine/chloroform, Oxon, sulfuric acid, formic acid, polyoxometalates, Hyamine, Na₂CaP₂O₇, Fe₃O₄ and K₂CO₃ [13-30]. However, most of these methods involve the use of expensive reagents, extended reaction times, harsh and drastic reaction conditions, the generation of a large amount of toxic waste and difficulty of reuse multiple times. At this point, the development of new eco-friendly synthesis methods that can be operated at mild conditions is the subject of interest in recent years. Thus, we thought it would be interesting to use the Animal Bone Meal (ABM) and its modified analog by impregnation with sodium nitrate (NaNO₃/ABM) as new catalysts for the oximes synthesis. On the other hand, it reported that the ABM and its modified analogs (with salts or Lewis acid) can catalyze several organic transformations such as crossed-aldol condensation [31]; thia-Michael addition [32]; synthesis of benzimidazoles, benzoxazoles, and benzothiazoles [33]; preparation of chalcones and aza-Michael adducts [34]; synthesis of a 2-amino-4H-chromene library by multi-component condensation [35] and synthesis of 3-cyanopyridine derivatives by multi-component reaction [36]. In continuation of our attempts to overcome health and environmental problems in organic synthesis and explore the catalytic activity of ABM and NaNO₃/ABM, we herein report an interesting method to oximes synthesis from the reaction of aldehydes or ketones with hydroxylamine hydrochloride (Scheme 1) using the ABM or its modified analog NaNO₃/ABM as heterogeneous, eco-friendly and recyclable catalysts under solvent-free conditions.



Scheme 1: ABM or NaNO₃/ABM catalyzed synthesis of oximes **3** in solvent-free conditions.

2. Experimental

2.1. Preparation of ABM and his doped analogs NaNO₃/ABM

Animal bones were collected from nearby butcher shops. All of the attached meat and fat were removed and cleaned from the bones. The bones were then washed several times with tap water at room temperature and left in open air for several days to get rid of odors. Later, they were transferred to the oven at 80 °C for drying. The dried bones were crushed and milled into different particle sizes in the range 45–200 μm then calcined for 2h at 800 °C. The residue was washed with water and was used after drying for 24h at 80 °C. The residue was washed with water and was dried overnight at 100 °C in a conventional drying oven, and then calcined at a heating rate of 2 °C/min to 400 °C, and kept at this temperature for 4h. The modified bones NaNO₃/ABM was prepared by impregnating the bones with an aqueous solution of sodium nitrate. The weight ratio used was NaNO₃/bones = 1/2. The mixture was stirred vigorously at room temperature, evaporated to dryness, dried, and calcined at 800 °C for 2h. The catalysts obtained were characterized by Differential Scanning Calorimetric (DSC) coupled with Thermogravimetric Analysis (TGA) (Figure 1), X-ray diffraction (Figure 2), Scanning electron microscopy with energy dispersive (SEM/EDS) (Figure 3 and 4), FT-IR (Figure 5) and Zero point charge pH.

2.2. Characterization of ABM and NaNO₃/AM

2.2.1. Thermal analysis (TGA and TDA)

The thermal gravimetric analysis was carried out on a TGA SHIMADZU DTG-60 Thermogravimetric in an alumina crucible, at a heating rate of 10 °C/min under air atmosphere. The mass of the samples was 12 mg. The sample pan was placed in the balance system equipment and the temperature was raised from 16 to 900°C.

2.2.2. XRD analysis

It provides information on the purity, crystallinity and values crystallographic parameters. The analysis by X-ray diffraction was performed on the powder in ambient conditions of temperature and pressure. The X-ray diffractometer used was a Panalytical diffractometer, equipped with a copper X-ray (wavelength $\lambda = 1.54 \times 10^{-10}$ m; tension V = 45 kV, intensity I = 35mA), and with a monochromator eliminating K β radiation.

The analyses were carried out using the classical θ -2 θ configuration, with 2 θ angle steps of 0.02° and counting times of 20 s per step.

2.2.3. SEM-EDS analysis

The scanning electron microscope (SEM) is used to obtain images of the surface of substantially all solid materials at scales ranging from that of the lens (x 10) of the transmission electron microscope (x 500000), its principle of operation is the interactions between the material and an electron beam. The instrument used is Supra 40 VP COLUMN GEMINI ZEISS coupled to an analyzer (Oxford Instruments X-Max 20 mm²) with EDXS detector (Energy Dispersive X-rays Spectroscopy) to determine the local quantitative elemental composition a sample with a maximum resolution of 1 micron at voltages ranging from 10 to 25 kV.

2.2.4. FTIR analysis

Fourier transformed infrared (FTIR) spectrum of the sample was recorded by Fourier transform infrared (Nicolet 6700 FT-IR, Thermo Scientific) spectrophotometer. The FTIR spectrum ranged from 4000 to 500 cm⁻¹ at a resolution of 4 cm⁻¹ by making an ATR mode.

2.2. General method of oximes preparation

1 mmol of aldehyde or ketone **1** and 1.5 mmol of hydroxylamine hydrochloride **2** were mixed with 0.1 g of the catalyst support, and the mixture was heated at 80 °C. After the completion of the reaction, the reaction mixture was washed with dichloromethane and the catalyst was removed by filtration.

The solution obtained was evaporated under reduced pressure. Further purification was accomplished by column chromatography on silica gel (60-120 mesh, eluted with a mixture of hexane and ethyl acetate ratio 2/10). The purified products were analyzed by melting points, ¹H NMR and IR spectroscopies.

3. Results and discussions

3.1. Thermal analysis

The curves of Thermogravimetric analysis (TGA) and corresponding flow profiles of heat from 16.25 °C to 900 °C. The thermogram samples generally show three successive stages of the weight loss; the first below 200 °C, the second between 200 and 600 °C and the third between 600 °C and 800 °C. Above 800 °C, the weight change is not significant [37-39]. The results of DSC showed an endothermic peak at 67.8 °C corresponding to loss of surface water and structural water followed by two exothermic peaks with a maximum around 359.66 °C corresponding to loss of collagen and a shoulder around 535.31 °C for loss of collagen and organic matter respectively [40] and at the end one small endothermic peak at 693.2 °C corresponding to loss of mineral CO₂ (Figure 1).

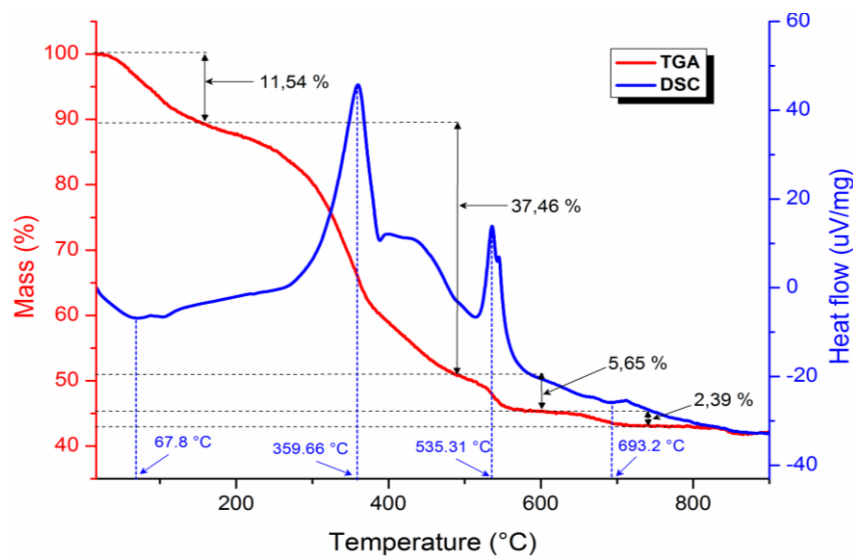


Figure 1: TGA and DSC plots of the control samples (non calcined bovine bone) in the 16.25–1000 °C temperature range.

3.2. XRD analysis

Figure 2a reports the XRD pattern of the ABM phase thermally calcined at 900 °C. First, these results confirm that the amorphous organic material was removed after calcination. Second, it should be recalled that the XRD analyses for ABM in the range $2\theta = 5-80^\circ$ clearly showed that the hydroxyapatite $\text{Ca}_{10}(\text{PO}_4)_6(\text{OH})_2$ powder was in a major structured form by comparison with the standards JCPDS data (96-901-0052) [41]. This identification allowed attributing (h k l) Miller indices to Bragg peaks, in conformity with the approximate parameters of a compact hexagonal $a = b = 9.4148 \text{ \AA}$, $c = 6.8791 \text{ \AA}$, $\alpha = \beta = 90^\circ$, $\gamma = 120^\circ$ [42] which was characterized with P63/m space group (N° 176).

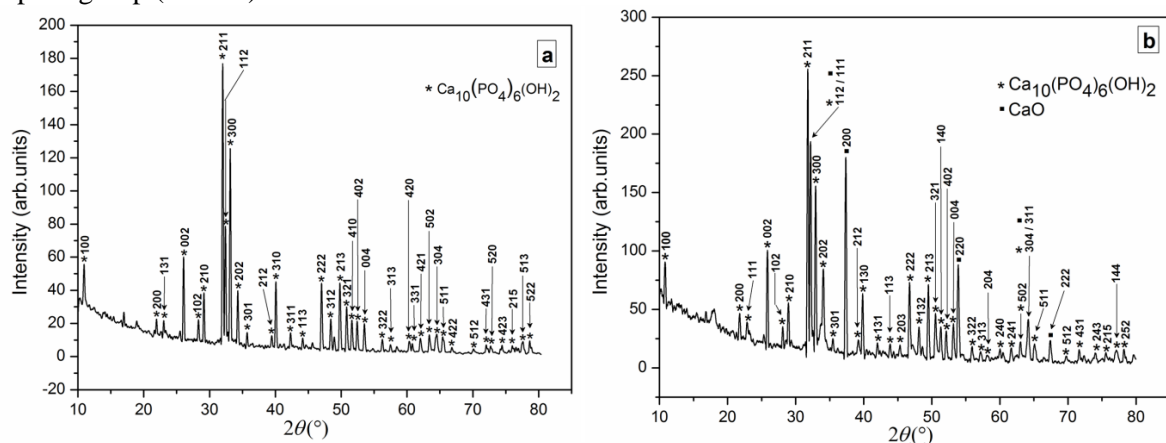


Figure 2: X-Ray of (a) ABM and (b) NaNO₃/ABM

The XRD pattern of NaNO₃/ABM sample is shown in Figure 2b. The diffraction rays characteristics of hydroxyapatite Ca₁₀(PO₄)₆(OH)₂ are identified; these rays are consistent with standard JCPDS (01-074-0565). This identification allowed attributing (h k l) Miller indices to Bragg peaks, in conformity with the approximate parameters of a compact hexagonal a = b = 9.4240 Å, c = 6.8790 Å, α = β = 90°, γ = 120° [43] which was characterized with P63/m space group (N° 176). In addition, the corresponding rays of calcium oxide CaO (standard JCPDS file 00-004-0777) which is comparable with cubic structure a = 4.8106 Å [44], characterized by Fm-3m space group (N° 225).

3.3. SEM-EDS analysis

The scanning electron analyses of ABM (Figure 3) show that its spherical morphology is characterized by small particles whose average size is between 0.2 to 1 μm (from images 3a and 3b). The images 3c and 3d show that these particles form agglomerates which have a size between 10 and 50 μm. These shapes showed the presence of a significant percentage of cavities (in all images) which will be interesting for the catalysis. EDS analysis was performed on a large of the ABM sample including small and large grains. The results of this analyze showed that the mean experimental atom fractions of the Ca and P heavy atoms were successively about 63 and 35 (in atomic %), (ignoring light atoms such as C, H and O, and relating to 100%), which gives a Ca/P ratio equal to 1.8 higher than that which characterizes the stoichiometric hydroxyapatite Ca₁₀(PO₄)₆(OH)₂ (1.67) and the others minor phases containing calcium Ca.

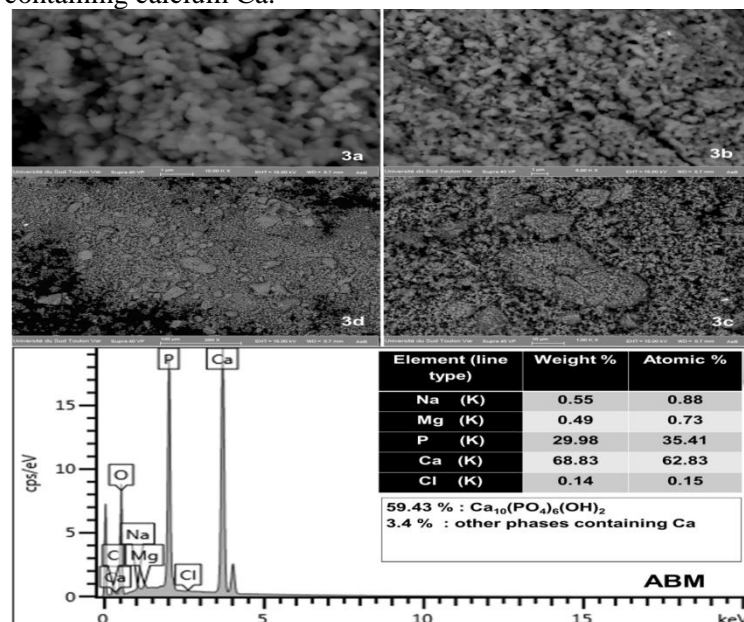


Figure 3: SEM images and EDX of ABM

In NaNO₃/ABM sample (Figure 4), the general morphology is characterized by agglomeration of spheroidal particles having regular sizes and shapes (0.3-1 μm) (from images 4a and 4b). The images 4a, 4b and 4c show that this shape would be very interesting for catalyze because of the amount of cavities observed. The NaNO₃/ABM EDS analyzes (Figure 4) were performed on a portion of the sample, including the small and large grains. It follows from this analysis that the average fraction of atoms Ca, P and Na are respectively about 75, 18 and 6 (in atomic %). The Ca/P ratio equal to 4.16 uppermost than 1.67 (stoichiometric hydroxyapatite), these results confirm those of XRD that showed the existence of two majority phases containing Ca (Ca₁₀(PO₄)₆(OH)₂ and CaO) with high percentages and the others minor phases containing calcium Ca.

3.4. Infrared analysis

The infrared analysis of the ABM (Figure 5) shows the characteristic bands of hydroxyapatite 563, 599, 963 cm⁻¹ (shoulder), 1028 cm⁻¹ (intense band) and 1092 cm⁻¹ (shoulder) due to hydroxyapatite vibrations (group PO₄⁻³) [45-47]. Carbonate group (CO₃⁻²) in the FT-IR spectra was identified by intense bands at 874 cm⁻¹ (small band) and broad band 1385–1635 cm⁻¹ (1415 and 1456 cm⁻¹) associated with out-of-plane bending mode and asymmetric stretching, respectively [46, 48]. As shown also, there are OH stretching (at 3657 cm⁻¹) and liberation bands (634 cm⁻¹) [46-49].

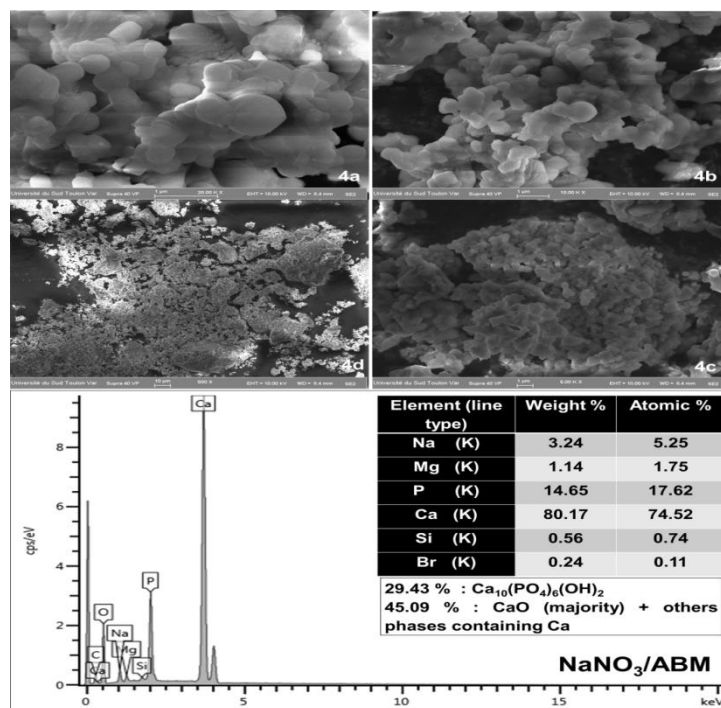


Figure 4: SEM images and EDX NaNO₃/ABM

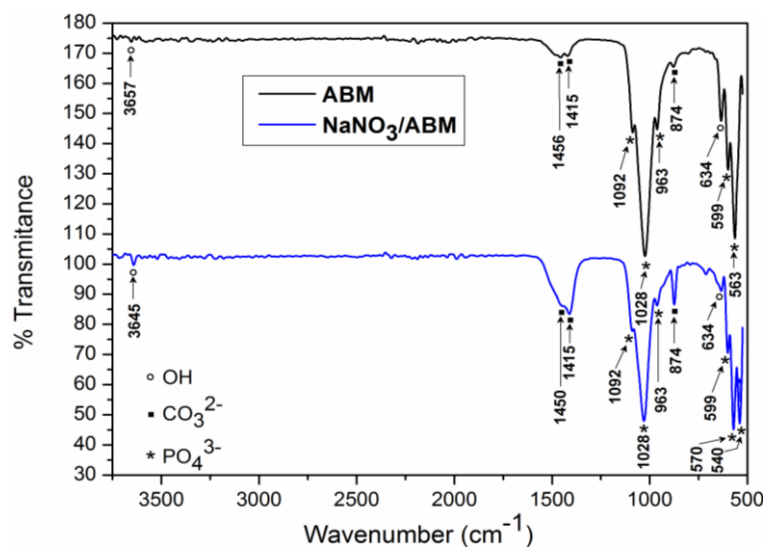


Figure 5: FT-IR spectra of ABM and NaNO₃/ABM

Infrared analysis of NaNO₃/ABM (Figure 5) clearly showed the same functional groups present in the ABM. Two limitations are observed: the first is the appearance of the corresponding new band PO₄³⁻ around 540 cm⁻¹, the second is the high intensity of corresponded CO₃²⁻ bands more than its analogues in the ABM, it which shows the appearance of other phases (CaO).

3.5. Optimization of the reaction

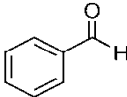
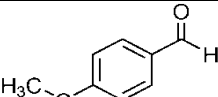
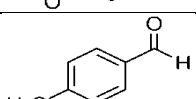
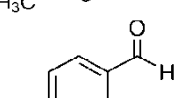
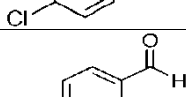
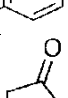
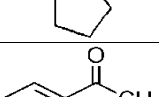
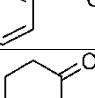
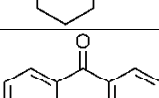
In order to explore the potential activity of these heterogeneous catalysts and to optimize the reaction conditions, the synthesis of compound **3a** was used as model reaction. Therefore, we initially investigated the reaction of benzaldehyde **1a** (1 mmol) with hydroxylamine hydrochloride **2** (1.5 mmol) in the presence of the different amounts of ABM or NaNO₃/ABM in free-solvent conditions at 80 °C. In the absence of these catalysts no product could be detected even after 60 min. However, in the presence of different amount of ABM or NaNO₃/ABM (0-0.2g), the reaction between benzaldehyde **1a** and hydroxylamine hydrochloride furnished the desired oximes **3a**. The best yield for this reaction was obtained for quantity greater than or equal to 0.1 g of both catalysts. Thus, we fixed the weight at 0.1 g because these results reveal that this amount of ABM (or

NaNO₃/ABM) provided the best effect of economy of catalyst charge and purity of products. Thereafter, we examined the effect of solvent in order to compare the solvent-free conditions with the solvent conditions; we performed the same reactions in seven solvents such as H₂O, EtOH, CH₃OH, CH₂Cl₂, CHCl₃, CH₃CN and C₃H₆O under reflux. We found that the ethanol was the best solvent which led to high yield 70% after 35 min with ABM and 81% with NaNO₃/ABM even after 5 min at 80 °C. However, the reaction proceeded under solvent-free conditions at 80 °C and led to the desired product **3a** in good yield 84% after 35 min with ABM and 94% with NaNO₃/ABM in only 5 min, this is because the dispersion and solvation of the reactants in the solvent prevents probably the contact with the surface of the two catalysts.

3.6. Oximes synthesis with others aldehydes and ketones

To assess the generality of this approach for the synthesis of oximes, various aromatic ketones and aldehydes were tested with these catalysts in the same reaction conditions, the results are summarized in Table 1.

Table 1: Summary of the various oximes using ABM and NaNO₃/AB as catalysts support

Entry	Aldehyde or ketone	Yield (%) / Time (min)	
		ABM	NaNO ₃ /ABM
1		84/25	94/5
2		86/25	96/5
3		84/25	94/5
4*		84/25	94/5
5		85/25	95/5
6		68/25	78/5
7		74/25	85/5
8		70/25	79/5
9		83/25	92/5

Reactions conditions: ketone or aldehyde (1 mmol) and hydroxylamine hydrochloride (1.5 mmol), 0.1 g of ABM or NaNO₃/ABM in free-solvent conditions at 80 °C

*Minimum amount of ethanol is used to solubilize the reactants.

From these results (Table 1), the use of the ABM unmodified leads to products **3** in good yields between 68% (entry 6) and 86% (entry 2) in solvent-free conditions, the completion reactions was reached after 25 min. Under similar conditions with NaNO₃/ABM, the yields are increased by almost 10% in each reaction (between 78 and 96%) and reaction times are reduced up to five times (5 min) with all products.

In general, the kinetic control in the presence of NaNO₃/ABM shows that these reactions are realized in very short time. Analysis of the spectral data of ¹H NMR showed that for all the prepared products, only E-isomers were formed.

The difference observed between ABM and NaNO₃/ABM it is probably due to the difference in the geometry of these catalysts. Indeed, an occurrence of new phases in the NaNO₃/ABM catalyst may play a role in catalysis. The only limitation observed is the difference in reactivity between aldehydes and ketones. Indeed, aldehydes are more reactive than ketones; this is due to steric genes presented in the case of ketones compared to aldehydes.

In the case of aromatic aldehydes **1**, the results indicate that these compounds with both electron-donating and electron-withdrawing substituents display high reactivity with hydroxylamine hydrochloride and generate the corresponding products **3** in good yields.

One of the key points to understand the reaction mechanism in heterogeneous catalysis is the determination of the active surface sites and the activation processes. In the case of the oximes synthesis, the reaction was mostly based on addition-elimination processes.

In the case of our work, the presence of negative and positive charges (CO₃²⁻, PO₄³⁻, Ca²⁺ and Na⁺) on the surface of the catalyst supports ABM and NaNO₃/ABM follows this process by having both acid and basic sites in the same lattice as in the case of apatite forms [50-52]. In this work, the pH levies during different reaction times shows a values between 4.5 and 6. In this pH realm, these catalyst supports are charged positively. This is confirmed by the point of zero charge (PZC) of the ABM (pH_{ZPC}= 8.43) and NaNO₃/ABM (pH_{ZPC}=11.56). In addition, the Ca/P ratio is greater than 1.65 in the case of the form of hydroxyapatite contained in the ABM and NaNO₃/ABM (Ca₁₀(PO₄)₆(OH)₂). In this case, hydroxyapatite's calcium-bearing c-faces were more highly exposed [52]. In the case of the form of CaO, calcium is more highly exposed in all the faces of the cube forming CaO.

From these results, a tentative mechanism for the catalyzed oximes preparation in the presence of ABM or NaNO₃/ABM is proposed involving the activation of aldehydes or ketones; the calcium cations acts as Lewis acid and play a significant role in increasing the electrophilic character of carbonyl carbon atom of the starting aldehyde or ketone and stabilizing the complex formed by the coordination of the oxygen lone electron pair. This activation facilitates the nucleophilic attack by the nitrogen of hydroxylamine hydrochloride on the carbonyl carbon atom of aldehydes or ketones. This reaction gave an unstable carbinolamine intermediate. This intermediate led to corresponding oximes by dehydration (Figure 6).

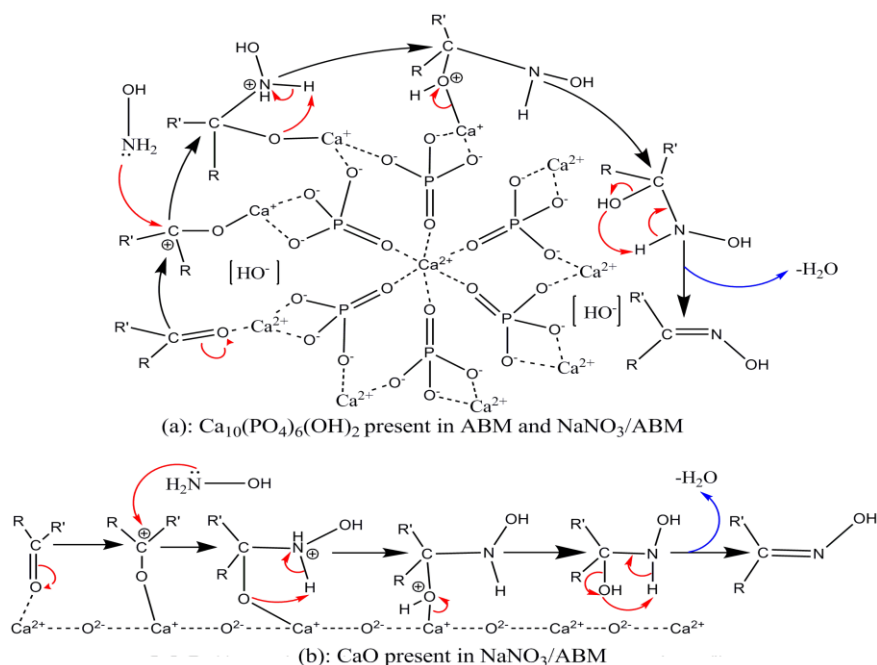


Figure 6: Synthesis mechanism of oximes by ABM and NaNO₃/ABM

The reusability of ABM and NaNO₃/ABM was examined in order to test their effectiveness for recycling. After each reaction, ABM and NaNO₃/ABM were readily separated, washed with acetone and regenerated by calcination at 500°C for 2h for each new reuse. Each reaction was carried out in the same conditions using benzaldehyde **1a** and produced the corresponding product **3a** in fairly good yield. The results of this study were presented in Figure 7 during eight repeated cycles.

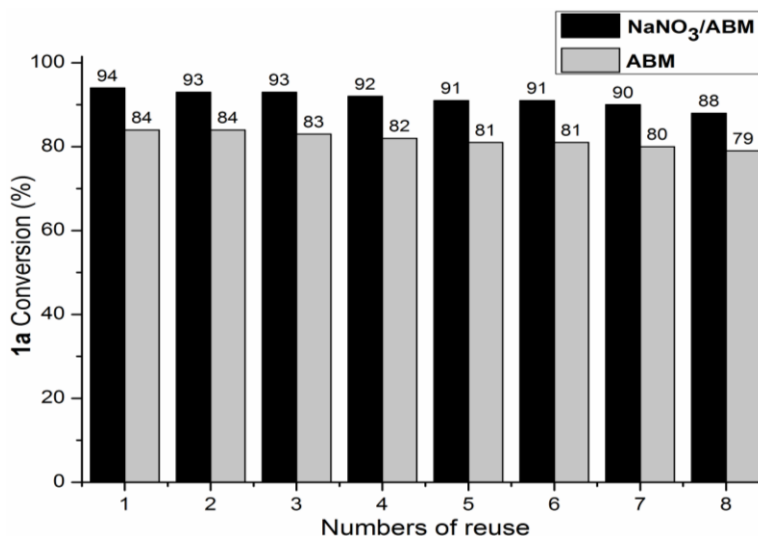


Figure 7: Reusability of ABM and NaNO₃/ABM in the oximes preparation

As shown in Figure 7, it should be noted that even in the eighth round, reuse of the catalysts recovered can produce the corresponding product **3a** in good yield. The conversion of benzaldehyde decreased from 94% to 88% using NaNO₃/ABM and from 84% to 79% using ABM after 8 times. The decrease of the reusability may be attributed to the loss of active sites after reaction

Conclusion

In summary, we have developed a simple and efficiently method for the oximes synthesis from aromatic aldehydes or ketones with hydroxylamine hydrochloride. The procedure for this synthesis is based on the use of ABM and NaNO₃/ABM as catalyst supports under free-solvent conditions that achieve high yields. The high product yields, operational simplicity, mild reaction conditions, short reaction times and recyclability as well as the environmental compatibility are the notable advantages of the present procedure. The novelty of the systems lies in their low cost and availability of the solid supports. Further studies in the application of these catalysts to other organic reactions are underway in our laboratory.

Acknowledgement-Authors are highly thankful to the “Association AIRS2D” for all kinds of help and funding.

Reference

1. Kassa J., Kuca K., Karasova J., Musilek K. *Mini-Rev. Med. Chem.* 8 (2008) 1134.
2. Curtis M.P., Chubb N., Ellsworth E., Goodwin R., Holzmer S., Koch J., McTier T., Menon S., Mills K., Pullins A., Stuk T., Zinser E., *Bioorg. Med. Chem. Lett.* 24 (2014) 501.
3. Kim Y., Hong Y.D., Joo Y.H., Woo B.Y., Kim S-Y., Koh H.J., Park M., Byoun K.H., Shin S.S., *Bioorg. Med. Chem. Lett.* 24 (2014) 2807.
4. Kim Y.S., Jung S.H., Park B-G., Ko M.K., Jang H-S., Choi K., Baik J-H., Lee J., Lee J.K., Pae A.N., Cho Y.S., Min S-J., *Eur. J. Med. Chem.* 62 (2013) 71.
5. Odz'ak R., Skocibušić M., Maravic A., *Bioorg. Med. Chem.* 21 (2013) 7499.
6. Chiang Y.H., *J. Org. Chem.* 36 (1971) 2146.
7. Liu K.C., Shelton B.R., How R.K., *J. Org. Chem.* 45 (1980) 3916.
8. Buehler E., *J. Org. Chem.* 32 (1967) 261.
9. Schoenewaldt E.F., Kinnel R.B., Davis P., *J. Org. Chem.* 33 (1968) 4270.
10. Ghiaci M., Aghaei H., Oroojeni M., Aghabarari B., Rives V., Vicente M.A., Sobrados I., Sanz J., *Cat. Commun.* 10 (2009) 1486.
11. Jin J., Li Y., Wang Z.J., Qian W-X., Bao W.L., *Euro. J. Org. Chem.* (2010) 1235–1238.
12. Flick A.C., Caballero M.J.A., Lee H.I., Padwa A., *J. Org. Chem.* 75 (2010) 1992.
13. Ramon R.S., Bosson J., Diez-Gonzalez S., Marion N., Nolan S.P., *J. Org. Chem.* 75 (2010) 1197.
14. Damljanovic I., Vukicevic M., Vukicevic R.D., *Monatshefte für Chemie.* 137 (2006) 301.
15. Kad G.L., Bhandari M., Kaur J., Rathee R., Singh J., *Green Chem.* 3 (2001) 275.

16. Sharjhi H., Sarvari M.H., *J. Chem. Res. (S)* (2000) 25.
17. Sharghi H., Hosseini M., *Synthesis*. 8 (2002) 1057.
18. Eshghi H., Hassankhani A., *Org. Prep. Proced.Int.* 37 (2005) 575.
19. Guo J.J., Jin T-S., Zhang S.L., Li T.S., *Green Chem.* 3 (2001) 193.
20. Li J.T., Li X.L., Li T.S., *Ultrason. Sonochem.*13 (2006) 200.
21. Hajipour A.R., Rafiee F., Ruoho A.E., *J. Iran. Chem. Soc.* 7 (2010) 114.
22. Sosnovsky G., Krogh J.A., Umhoefer S.G., , *Synthesis*. (1979) 722–724.
23. Xia J-J., Wang G-W., *Molecules* 12 (2007) 231.
24. Weissmermer K., Arpe H., *J. Indian Org. Chem.* (1978) 222–225.
25. Olah G.A., Keumi T., *Synthesis* (1979) 112–113.
26. Sloboda-Rozner D., Neumann R., *Green Chem.* 8 (2006) 679.
27. Lad U.P.,Kulkarni M.A., Patil R.S., *RĀSAYAN J. Chem.* 3 (2010) 425.
28. Elmakssoudi A., Abdelouahdi K., Zahouily M., Clark J., Solhy A., *Catal.Comm.*29 (2012) 53.
29. Zeynizadeh B., Karimkoshteh M.J., *Nanostuct. Chem.* 3 (2013) 1.
30. Kim B.R., Sung G.H., Kim J-J., Yoon Y-J., *J. Korean Chem. Soc.* 57 (2013) 295.
31. Riadi Y., Mamouni R., Azzalou R., BoulahjarR., Abrouki Y., El Haddad M., Routier S., Guillaumet G., Lazar S., *Tetrahedron Lett.* 51 (2010) 6715.
32. Riadi Y., Mamouni R., Abrouki Y., El Haddad M., Saffaj N., El Antri S., Routier S., Guillaumet G., Lazar S. *Lett. Org. Chem.* 7 (2010) 269.
33. Riadi Y., Mamouni R., Azzalou R., El Haddad M., Routierd S., Guillaumet G., Lazar S. *Tetrahedron Lett.* 52 (2011) 3492.
34. Riadi Y., Abrouki Y., Mamouni R., El Haddad M., Routier S., Guillaumet G., Lazar S. *Chem. Cent. J.* 6 (2012) 1.
35. Riadi Y., Abrouki Y., Mamouni R., El Haddad M., Routier S., Guillaumet G., Lazar S. *Inter. J. Chem.* 2 (2013) 2051.
36. Riadi Y., Mamouni R., Routier S., Guillaumet G., Lazar S. *Environ Chem.Lett.*12 (2014) 253.
37. Haberko K., Bucko M.M., Brzezinska-Miecznik J., Haberko M., Mozgawa W., Panz T., Pyda A., Zarebski J. *J. Eur. Ceram. Soc.* 26 (2006) 537.
38. Etok S.E., ValsamiJones E., Wess T.J., Hiller J.C., Maxwell C.A., Rogers K.D., Manning D.A.C., White M.L., Lopez-Capel E., Collins M.J., Buckley M., Penkman K.E.H., Woodgate S.L., *J. Mater. Sci.* 42 (2007) 9807.
39. Mkukuma L.D., Skakle J.M.S., Gibson I.R., Imrie C.T., Aspden R.M., Hukins D.W.L., *Calcif. Tissue Int.* 75 (2004) 321.
40. Figueiredo M., Fernando A., Martins G., Freitas J., Judas F., Figueiredo H., *Ceramics Inter.* 36 (2010) 2383.
41. Powder Diffraction File PDF data base sets, JCPDS, International Center for Diffraction Data, Swathmore, PA USA (1994).
42. Verbeek R.M.H., Thun H.P., Driessens F.C.M., *Ber. Bunsenges Phys. Chem.* 84 (1980) 159.
43. Sudarsanan K., Young R.A., *Acta Crystallogr. Sect. B: Struct. Crystallogr.Cryst. Chem.* 25 (1969) 1534.
44. McMurdie H.F., Morris M.C., Evans E.H., Paretzkin B., Wong-Ng W., Hubbard C., *Powder Diff.* 1 (1986) 265.
45. Obadiah A., Swaroopa G.A., Kumar S.V., Jeganathan K.R., Ramasubbu A., *Bioresource Tech.* 116 (2012) 512.
46. Zaragoza D.L., Guzmán E.T.R., Gutiérrez L.R.R., *J. Miner. Mater. Charact. Eng.* 8 (2009) 591.
47. Markovic M., Fowler B.O., Tung M.S., *J. Res. Natl. Inst. Stand. Technol.* 109 (2004) 553.
48. Huang Yi-C., Hsiao P-C. Chai H-J., *Ceramics Inter.* 37 (2011) 1825.
49. Barakat N.A.M., Khil M.S., Omran A.M., Sheikh F.A., Kim H.Y., *J. Mat. Proces.Tech.* 209 (2009) 3408.
50. Bett J.A.S., Hall W.K., *J. Cat.* 10 (1968) 105.
51. Kibby C.L., Hall W.K., *J. Cat.* 31 (1973) 65.
52. Tsuchida T., Kubo J., Yoshioka T., Sakuma S., Takeguchi T., Ueda W., *J. Catal.* 259 (2008) 183.

(2016) ; <http://www.jmaterenvironsci.com/>